

DEVELOPMENT OF A HYDRODUCT

By

R. G. Anderson, Lt. Comdr. U. S. Navy  
C. W. Rush, Jr., Lt. Comdr. U. S. Navy  
T. R. McClellan, Lieut. U. S. Navy

In Partial Fulfillment of the Requirements  
for the Professional Degree in  
Aeronautical Engineering

California Institute of Technology  
Pasadena, California

1947

## TABLE OF CONTENTS

I. References	ii
II. Summary	iii
III. Acknowledgment	iv
IV. Introduction	1
V. Description of Apparatus	3
VI. Test Procedure	6
VII. Symbols	7
VIII. Analysis and Discussion	8
IX. Results	16
X. Conclusion	21
XI. Sample Data and Illustrations	24

REFERENCES

Air Technical Service Command,  
"Jet Propulsion", Chapter XV.

## SUMMARY

This report presents the results of experiments on a device for producing thrust for underwater propulsion. The principle of the device is based on accelerating a large mass of water by expansion of a small mass of gas, the gas being injected continuously into the water. The investigation consisted of tests conducted on ducts of several different designs; varying the exit area of the ducts, the water and gas flow, and the method of injecting and mixing the gas and water.

Using hydrogen gas at a rate of 0.0165 lbs/sec at a water flow rate of 27.4 lbs/sec, a maximum gross thrust of 29.2 lbs was obtained. At this water flow rate the internal friction drag of the duct was 20.5 lbs, giving a net thrust of 8.7 lbs. The effective exhaust velocity for these flow rates was 56,900 ft/sec. This is equivalent to a specific impulse of 1,770 sec., whereas a good conventional rocket fuel would have a specific impulse of about 250 sec. At low gas flow rates an effective exhaust velocity of 296,000 ft/sec. was obtained. However, at this low gas rate the gross thrust was less than the internal friction drag of the duct.

Effective exhaust velocity is defined as gross thrust divided by the mass flow rate of gas, and has the dimensions of velocity.

#### ACKNOWLEDGMENT

The authors wish to express their appreciation to Mr. C. Dodge and the Hydrodynamics section of the Jet Propulsion Laboratory for assistance in performing the experiments and to Mr. W. D. Rannie for technical advice.

## INTRODUCTION

The desirability of a device for underwater propulsion using direct gas injection is analogous to the desirability of the ramjet for propulsion in the atmosphere. Propellers for underwater propulsion are limited by cavitation which occur at excessive tip speeds. Conventional rockets are not ideal for underwater propulsion since all of the mass expelled must be carried within the rocket. For efficient high speed propulsion then, a device is needed which uses a small mass of self-contained fuel to accelerate a large mass of ambient fluid. In the ramjet the ambient fluid is air, while in the hydroduct it is water. The hydropulse is based on the same principle as the hydroduct, but operates intermittently instead of continuously.

The purpose of the investigation covered by this report was to determine a design for a hydroduct which would produce an effective thrust. In order to accomplish this purpose, ducts of several different shapes and dimensions were tested. The experimental results obtained were then compared with theoretical values to determine the relative effectiveness of each design. For gas rates at which positive net thrust was produced, experimental values were very much lower than theoretical. Therefore, various methods of increasing the performance at high gas rates were investigated. These methods were: increasing the water flow rate, injecting the gas so that proper mixing would take place, installing devices to promote turbulence in the mixing section, and adding de Laval nozzles to the exit section.

Further investigation is necessary to determine the optimum design

for a hydroduct. It is believed that further experiments will bring the performance at high gas rates closer to theoretical values.

Other investigations have been made on the hydroduct principle. The preliminary theoretical work was done by Dr. J. V. Charyk, Jet Propulsion Laboratory-GALCIT, Progress Report No. 2-2, 6 November 1943. Some Test work was done by Comdr. J. J. Baranowski, U.S.N. and Lt. Comdr. D. A. Seiler, U.S.N., using a duct of fixed design and varying the water and gas flow. R. C. Brumfield has written a technical memorandum for the Underwater Ordnance Division, NOTS, concerning the hydroduct for torpedo propulsion.

This investigation was conducted at the Hydrodynamics Section of the Jet Propulsion Laboratory, California Institute of Technology, Pasadena, California.

## DESCRIPTION OF APPARATUS

The apparatus used in performing the experiments may be divided into four general subdivisions:

- (1) The hydroduct body.
- (2) The water supply system.
- (3) The thrust measuring device.
- (4) The gas supply system.

The hydroduct bodies (figures 1a, 1c, 5a, and 8) consisted of three major parts; the entrance and diffusing section, the gas injection and mixing section and the contracting section with outlet nozzle. All sections were made of lucite to afford observation of the fluid flow. Three different diffuser sections (figures 1a, 1c, and 8) were used to obtain data for determining the effect of this section on the overall performance of the duct. Figure 1b shows the location of the eight 1/4-inch gas supply tubes on the periphery of the gas injection and mixing section. Inside the mixing section various types of devices for inducing turbulence were used. These are shown in figures 5b, 5c, and 5d. Figure 5b shows a grid of evenly spaced cylindrical bars. Figure 5c shows beads strung on wires to form a uniform pattern of spheres. Figure 5d shows a combination injector and "turbulator". The contracting section had a 2" inside diameter exit nozzle. To vary the exit area, nozzles having 1" .62 and 1" .44 inside diameters could be secured to the 2" section. The hydroduct body in figure 8 also provided for the attachment of de Laval nozzles to the 1" .44 exit section. Pressure gages were located at the entrance, injection, and outlet sections.



The water supply to the duct was obtained from a 4" diameter main. This was reduced to a 2" diameter and finally to a 1" diameter at the entrance of the duct. A gate valve in the main line was used to control the water flow. The rate of flow was indicated by a mercury manometer which measured the pressure drop across a calibrated orifice. Calibration curves of manometer readings vs. water flow in gallons per minute were plotted to obtain the mass rate of flow. The orifice plate used was designed to measure flow rates from 60 to 220 gallons per minute, giving an approximate maximum inlet velocity of 90 ft/sec.

The duct was mounted in a cradle, figure 18, which rolled on and was guided by ball bearings. The thrust measuring device was attached to the cradle. Thrust was measured by the deflection of a sylvon bellows-spring combination, figure 18. The volumetric change inside the bellows actuated a column of liquid in a manometer from which the thrust could be readily obtained. As shown in the figure, two sylvon bellows were used in order to measure the thrust when it was less than or greater than the drag produced by the water flowing through the duct.

The gas supply system consisted of three main parts; the gas weighing device, the gas flow rate control devices, and the gas injectors in the duct. The gas weighing device consisted of a beam balance resting on a knife edge. The gas supply bottle was mounted on one end of the balance, and compensating weights on the other end. (Figure 12). As gas was used from the bottle, the movement of the balance was recorded by means of a micrometer dial indicator. The difference in readings of the dial before and after a run gave the weight of gas used. Calibration curves of dial

reading vs. pounds of gas were made for use in calculations. The accuracy of the device was high since one division on the micrometer represented 0.65 grams of gas. The connections to the gas bottle for refilling were permanent fittings. These lines were so attached that they were free to move with the balance, and their only effect was to slightly damp its motion. The time for each run was recorded with a stop watch and thus the average mass rate of flow during the run was determined.

The gas from the supply bottle passed through a dehydrator made of porous metal and containing potassium hydroxide, and then through a pressure regulator into the injector supply manifold. The manifold had one inlet stop valve and separate stop valves for the eight gas supply lines leading to the injectors. This system provided a very flexible and effective control for the gas supply to the duct. The injectors used were of three main types; the perforated type shown in figure I section C-C, the open end type shown in figure I section B-B, and the porous metal type shown in figure 1b. The perforated type has gas outlet holes drilled in diametrically opposite lines along the sides of the tubes. The tubes could be rotated so that the gas flow could be directed in any desired direction relative to the water flow in the duct. The open end type was not perforated and permitted only  $\frac{1}{4}$ " diameter gas outlet at the distal end of the tube. The porous metal type consisted of a hollow thin walled gas chamber made of porous bronze. Gas from inside this chamber passed through the minute passages in the porous walls into the mixing section of the duct.

## TEST PROCEDURE

The procedure for conducting a test or run may be listed in the following steps:

- (1) Open water main gate valve and establish desired water flow rate through duct.
- (2) Adjust gas pressure to give desired flow rate of gas.
- (3) Record the following readings:
  - (a) Water flow manometer.
  - (b) Dial indicator on gas weighing device.
  - (c) Thrust manometer.
  - (d) Pressure at entrance, injection, and outlet sections of the duct.
- (4) Open individual gas injector stop valves.
- (5) Open stop valve to gas manifold and start watch simultaneously.
- (6) Record the following readings:
  - (a) Water flow manometer.
  - (b) Thrust manometer.
  - (c) Pressure at entrance, injection, and outlet sections of the duct.
  - (d) Gas regulator pressure.
- (7) Make visual observation of fluid flow and mixing during run.
- (8) At end of run close stop valve to gas manifold; stop watch.
- (9) Record the following readings:
  - (a) Time of run.
  - (b) Dial indicator on gas weighing device.
  - (c) Thrust manometer.
  - (d) Water flow manometer.

## SYMBOLS

Subscript 1 refers to conditions at inlet of hydroduct.

Subscript 2 refers to conditions at end of diffuser before gas is injected.

Subscript 3 refers to conditions at mixing section after gas is injected.

Subscript 4 refers to conditions at exit of hydroduct.

Subscript f refers to water.

Subscript g refers to gas.

No subscript denotes conditions at any arbitrary section.

F - Thrust (lbs.)

$u_{\text{eff.}}$  - Effective exhaust velocity  $\left(\frac{F}{Mg}\right)$  (ft./sec.)

u - velocity (ft/sec)

p - pressure (lb/in<sup>2</sup>)

T - Temperature (° R.)

$\rho$  - Density (slug ft<sup>3</sup>)

R - Engineering gas constant  $\left(\frac{\text{BTU}}{\text{slug } ^\circ\text{R}}\right)$

$R_g = \frac{R}{m_g}$

A - Area of cross section (ft<sup>2</sup>)

V - Volume (ft.<sup>3</sup>)

m - Molecular weight (lbs)

M - Mass (slugs)

$\mu$  - Mass ratio of gas to water  $\left(\frac{M_g}{M_f}\right)$

$\alpha$  - Dynamic pressure-static pressure ratio  $\left(\frac{\rho_s u_s^2}{2 p_s}\right)$

$\delta$  - Gas-water volume ratio  $\left(\frac{\mu \rho_g}{\rho_{g+}}$

$a_m$  - Velocity of sound in mixture of gas and water.

$a_g$  - Velocity of sound in gas.

## ANALYSIS AND DISCUSSION

In this analysis the following assumptions are made.

- (1) The gas obeys the laws of a perfect gas.
- (2) The liquid is incompressible.
- (3) Frictional losses are neglected.
- (4) Mixing is perfectly completed in the gas injection and mixing section.
- (5) The velocity in the mixing section is negligible.
- (6) The thermodynamic process of the mixture is adiabatic and is equivalent to the isothermal expansion of the gas alone.\*
- (7) The pressure at the entrance section ( $P_1$ ) equals the pressure at the exhaust nozzle ( $P_4$ ).
- (8) The pressure of the gas and the mixture are the same.

\* Reference: Jet Propulsion (Air Technical Service Command) page 502.

A.. Entrance and Diffuser Section

Fundamental equations:

$$(a) \rho u A = M$$

$$(b) P + \frac{\rho u^2}{2} = \text{constant}$$

From (a) and (b)

$$\rho_1 u_1 A_1 = \rho_2 u_2 A_2$$

Since  $\rho_1 = \rho_2 = \rho_f = \text{constant}$

$$u_2 = u_1 \frac{A_1}{A_2}$$

$$P_1 + \frac{1}{2} \rho_1 u_1^2 = P_2 + \frac{1}{2} \rho_2 u_2^2$$

$$I \quad P_2 = P_1 + \frac{\rho_f u_1^2}{2} \left[ 1 - \left( \frac{A_1}{A_2} \right)^2 \right]$$

The diffuser efficiency ( $\eta$ ) must also be considered.

$$\eta = \frac{P_2 (100)}{P_1 + \frac{1}{2} \rho_f u_1^2}$$

$$II \quad \eta \left( P_1 + \frac{1}{2} \rho_f u_1^2 \right) = P_2 (\text{actual})$$

B. Gas Injection and Mixing Section

$$\text{Let } M = M_g + M_f \quad \text{and} \quad \mu = \frac{M_g}{M_f}$$

$$\text{Now } \rho = \frac{M}{V} = \frac{M_g + M_f}{\frac{M_g}{\rho_g} + \frac{M_f}{\rho_f}}$$

$$\text{III } \frac{1}{\rho} = \frac{1}{\mu+1} \left[ \frac{1}{\rho_f} + \frac{\mu}{\rho_g} \right] \quad \text{which}$$

is the general expression for the density of the mixture. It is well to note at this point that all terms on the right side of equation III are constant except for  $\rho_g$ . Since  $\rho_g = \frac{p}{RT_g}$ , where  $P$  is the only pressure acting in the mixture and is assumed to equal the pressure of the gas, equation III becomes

$$\text{IV } \frac{1}{\rho} = \frac{1}{\mu+1} \left[ \frac{1}{\rho_f} + \frac{\mu R_g T_g}{p} \right]$$

Since the heat capacity of the liquid is much greater than that of the gas, and since the gas is injected as small bubbles which give instantaneous heat transfer from the liquid to the gas; the temperature of the mixture may be assumed to be constant and equal to the water temperature. Therefore equation IV gives a direct relation between the pressure and density of the mixture.

$$\text{From } \rho_3 u_3 A_3 = M ; \rho_2 u_2 A_2 = M_f ; A_3 = A_2$$

$$\text{We obtain } u_3 = \frac{M}{\rho_3 A_3} = \frac{M_f}{\rho_f A_2} \left[ 1 + \frac{\mu \rho_f}{\rho_g} \right]$$

$$\text{V } u_3 = u_2 \left[ 1 + \mu \frac{\rho_f}{\rho_g} \right]$$

From the momentum equation:

$$p_3 = p_2 + \rho_f u_2^2 \left[ 1 - \frac{\rho_3 u_3^2}{\rho_f u_2^2} \right]$$

$$p_3 = p_2 + \rho_f u_2^2 \left[ 1 - (1+\mu) \left( 1 + \frac{\rho_f}{\rho_g} \right) \right]$$

From the equations III and V and continuity

$$\text{VI } p_3 = p_2 + \rho_f u_1^2 \left( \frac{A_1}{A_2} \right)^2 \left[ 1 - (1+\mu) \left( 1 + \frac{\rho_f}{\rho_g} \right) \right]$$

C. Exit Nozzle Section

From Newton's law of motion and neglecting friction,

$$u du = - \frac{dp}{\rho}$$

Since  $\frac{1}{\rho} = \frac{1}{\mu+1} \left[ \frac{1}{\rho_f} + \mu \frac{R_g T_g}{p} \right]$ ,

$$u du + \frac{dp}{\mu+1} \left[ \frac{1}{\rho_f} + \mu \frac{R_g T_g}{p} \right] = 0$$

As discussed before, the pressure term **is** a variable and is assumed to follow a thermodynamic process which is isothermal.

From  $\frac{p_3}{\rho_{g3}} = \frac{p}{\rho_g} = R_g T_g$

Substituting for constant  $R_g T_g$

VII  $u du + \frac{dp}{\mu+1} \left[ \frac{1}{\rho_f} + \frac{\mu p_3}{\rho_{g3} p} \right] = 0$

Upon integrating the above between  $P_3$  and  $P_4$  the following result is obtained.

$$u_4^2 = u_3^2 + \frac{2}{\rho_f (\mu+1)} [p_3 - p_4] + \frac{2\mu}{\mu+1} \frac{p_3}{\rho_{g3}} \ln \frac{p_3}{p_4}$$

Since  $u_3 \sim 0$

$$u_4^2 = \frac{2}{\rho_f} [p_3 - p_4] + \frac{2\mu}{\mu+1} \frac{p_3}{\rho_{g3}} \ln \frac{p_3}{p_4}$$

But  $p_4 = p_1$

and  $\frac{2}{\rho_f} [p_3 - p_1] \cong \frac{u_1^2}{\mu+1}$

$$\frac{p_3}{p_1} = 1 + \frac{1}{2} \frac{\rho_f u_1^2}{p_1} - \frac{1}{2} \rho_{g3} u_3^2 \left( \frac{1}{p_1} \right)$$

$$\frac{p_3}{p_1} \cong 1 + \frac{1}{2} \frac{\rho_f u_1^2}{p_1}$$



$$\text{So: } \left(\frac{u_0}{u_1}\right)^2 = \frac{1}{\mu+1} \left[ 1 + \frac{2\mu \rho_3}{u_1^2 \rho_{g3}} \{n. (1 + \frac{\rho_f u_1^2}{2\rho_1})\} \right]$$

$$\text{Let } \alpha = \frac{\rho_f u_1^2}{2\rho_1}$$

$$\delta = \mu \frac{\rho_f}{\rho_{g4}}$$

$$\text{and since } \frac{\rho_3}{\rho_{g3}} = \frac{\rho_4}{\rho_{g4}} = \frac{\rho_1}{\rho_{g4}}$$

$$\text{VIII } \left(\frac{u_0}{u_1}\right)^2 = \frac{1}{\mu+1} \left[ 1 + \frac{\delta}{\alpha} \{n. (1 + \alpha)\} \right]$$

The thrust of the hydroduct is

$$F = (M_g + M_f) u_0 - M_f u_1$$

To express the effective exhaust velocity in a convenient manner for comparison with a rocket motor.

$$u_{\text{eff.}} = \frac{F}{M_g} = \frac{\mu+1}{\mu} u_0 - \frac{u_1}{\mu}$$

Substituting equation VIII in the above,

$$\text{IX } u_{\text{eff.}} = \frac{u_1}{\mu} \left[ \sqrt{(\mu+1) \left[ 1 + \frac{\delta}{\alpha} \{n. (1 + \alpha)\} \right]} - 1 \right]$$

$$\text{Effective Area Ratio} = \frac{A_0}{A_1}$$

$$\frac{1}{\rho_4} = \frac{1}{\mu+1} \left[ \frac{1}{\rho_f} + \frac{\mu}{\rho_{g4}} \right]$$

$$\rho_f (\mu+1) A_1 u_1 = \rho_4 A_0 u_0$$

$$\frac{A_0}{A_1} = \frac{u_1}{u_0} \left[ 1 + \frac{\mu \rho_f}{\rho_{g4}} \right]$$

$$x \frac{A_2}{A_1} = \frac{u_1}{u_2} [1 + \delta]$$

A plot of  $A_2/A_1$  and  $\delta$  is shown in figure 11 from which the optimum area ratios for a given  $\delta$  can be obtained.

D. Calculation of the Speed of Sound in the Mixture. ( $a_m$ )

From the general equation of the density of the mixture.

$$\frac{1}{\rho} = \frac{1}{\mu+1} \left[ \frac{1}{\rho_f} + \mu \frac{R_g T_g}{p} \right]$$

$$-\frac{1}{\rho^2} \frac{d\rho}{dp} = \frac{1}{\mu+1} \left[ \mu R_g \frac{d}{dp} \left( \frac{T_g}{p} \right) dp \right]$$

Before the differentiation can be completed a thermodynamic process for the gas must be assumed. Two different cases will be considered.

(1) Isothermal ( $T_g = \text{constant}$ )

$$a^2 = \frac{\mu+1}{\mu} \left[ \frac{p^2}{R_g T_g} \right] \left( \frac{1}{\rho} \right)^2$$

$$= \frac{\mu}{\mu+1} \left( \frac{a_g^2}{\gamma} \right) \left( 1 + \frac{\rho_g}{\mu \rho_f} \right)^2$$

Where  $\gamma$  = ratio of specific heats for the gas.

For the section of interest, the exhaust section.

$$XI \quad a_m = a_g \sqrt{\frac{\mu}{\mu+1} \left( \frac{1}{\gamma} \right) \left[ 1 + \frac{1}{\delta} \right]}$$

(2) Adiabatic process

By differentiation as before:

$$XII \quad \frac{a_m}{a_g} = \sqrt{\frac{\mu}{\mu+1} \left[ 1 + \frac{1}{\delta} \right]}$$

in the exhaust section.

For hydrogen gas at standard conditions and  $\mu$  of .0054, the computed speeds of sound in the mixture are 70 ft/sec. for isothermal assumptions and 83 ft/sec. for adiabatic assumptions. These values correspond to a  $\beta$  of .603 as shown in figure 13. At first these values seem to low, since the speed of sound is high in both water and hydrogen. With the following reasoning however it is seen that sonic velocity is low in the mixture.

The water is incompressible, the gas is compressible; therefore the elastic properties of the mixture are determined by the gas. The mass of the mixture is determined by the liquid. This gas is analogous to a spring with a given spring constant "k" which is loaded with a small mass "m" equal to the mass of the gas. Loaded in this manner the frequency is:

$$f_1 = \sqrt{\frac{k}{m \cdot g}}$$

Now consider the load on the spring increased by an amount equal to the mass of the water "M". The spring constant frequency now because:

$$f_2 = \sqrt{\frac{k}{m_g + m}}$$

which is much lower than the former value because of the added mass and the elasticity of the spring. Such is the case in the mixture of gas and water. The velocity of sound is greatly reduced by the elasticity of the gas and the mass of the water.

One other effect can be seen from the equations for the speed

of sound as derived. As  $\mu$  increases  $\delta$  will also increase. In other words, as the ratio of the mass of gas to the mass of liquid increases the ratio of the volume of gas to the volume of liquid increases. The effect on the speed of sound with increasing  $\delta$  is given in figure 13.

Figure 13 also shows the variations of theoretical exhaust velocity  $U_4$  with increasing  $\delta$ . The maximum values of  $\delta$  for  $U_4$  less than sonic velocity are 0.15 and 0.3 for the isothermal and adiabatic equations respectively. Experimental results, shown in figure 7, indicate a maximum value of approximately 0.4 for  $\delta$  before the choking effect of sonic velocity in the exit section reduces the overall performance. Since the experimental value checks closely with the adiabatic equation for the speed of sound in a mixture, the adiabatic assumption must very closely approach actual conditions.

## RESULTS

In order to simulate a hydroduct moving through the water a free stream of water was allowed to enter the model. This method was adopted because of the ease of taking data and because no towing carriage was available for moving the duct through the water. It is somewhat different from forcing water into the entrance by some device, such as a flexible hose rigidly clamped to the duct. If the latter were done the duct would be similar to the nozzle of a hose in that no matter what pressure gradients were built up, the exit end of the duct would be the only means of escape. On the other hand pressure occurring in a hydroduct moving through the water might force part of the water out through the entrance instead of the exit. By not having any connection between the water pipe and the entrance actual conditions were simulated as closely as possible. In some runs both water and gas were forced out of the forward end of the duct.

Three diffuser sections were tested. The short, wide-angle diffuser shown in figure Ia, did not give good pressure recovery. When sufficient gas was injected into the mixing section however, enough back pressure was built up in the diffuser to prevent separation of flow from the wall. Under these conditions there was sufficient pressure recovery from the inlet to the injection section to obtain a satisfactory expansion of the gas in the outlet nozzle. The disadvantage of obtaining pressure by this means was that the pressure in the diffuser section forced part of the gas and water out through the entrance of the duct. The advantage of this type of diffuser was that large scale turbulence was produced in the mixing section.

This turbulence caused complete mixing of the gas and water. The efficiency of the diffuser shown in figure 1c was quite high, the pressure recovery being approximately 90%. This diffuser did not produce turbulence in the mixing section however. Since the stream velocity at the mixing section was only about 3 ft/sec at a water rate of 27.4 lbs/sec, the gas bubbles were allowed sufficient time to rise and collect in the upper part of the duct, with a resulting decrease in performance of the duct (Figure 16).

In order to obtain both pressure recovery and good mixing conditions, various devices for producing turbulence were installed in the diffuser and the mixing section. Figure 1c shows a 2 1/2" I.D. steel pipe with a flange at one end. The turbulence caused by water from the pipe entering the 5".25 diameter mixing section was comparable to the turbulence produced by the diffuser of figure 1a. However, in this case water and gas were not forced out the entrance to the duct. The disadvantages of the pipe were that it decreased the length of the diffuser and increased the frictional drag of the duct. Figure 5 shows devices which were installed in the mixing section to induce turbulence. Figure 6 shows the results obtained using these "turbulators". At a gas to water volume ration of 2.0, for hydrogen gas the gross thrust obtained using the pattern of spheres was 15.4 lbs. compared to a gross thrust of 13.2 lbs. using the grid of 1/4" tubes under the same conditions. For the same conditions, but with no "turbulator" installed, the gross thrust was only 11.9 lbs.

Figure 3 indicates the results of experiments to determine the effects of bubble size of the gas injected on the performance of the

duct. Four types of injectors shown in figure 1b were tested at both high and low water rates. The open end  $1/4$ " tubes gave the largest bubble size. Tubes with  $1/32$ " holes drilled along the sides gave the next largest bubbles. Tubes with No. 79 holes gave very small bubbles. Porous metal injectors produced numerous streams of fine bubbles. At low gas rates (rates for which a positive net thrust was not obtained) the results were scattered. Contrary to what might be expected, the open end tubes which produced the largest bubbles gave the highest value of effective exhaust velocity. At high gas rates there was very little difference between the results obtained using the various injectors, indicating that for practical purposes the size of bubbles injected is not critical.

Two general types of converging nozzles were used in the exit suction. The first type shown in figure 5a, had a small included angle and gave very smooth flow. Its length however was approximately one half the total duct length. As a result of this length and slow convergence, velocity increased relatively slowly from the mixing section to the exit and gas bubbles had time to rise. Large accumulations of gas in the top of the duct caused uneven performance.

As a result of these experiments a second exit section was designed (figure 8). It had a much greater included angle which with its length of about one fourth total duct length causing very rapid velocity increase. With this short length and rapid convergence, bubbles had no time to rise and smooth performance resulted. Other performance factors were not affected by the shape of the convergent section.

Various ratios of entrance area to exit area were tested always

maintaining the exit area ( $A_4$ ) greater than the entrance area ( $A_1$ ). As was expected, using large ratios of  $A_4/A_1$  caused an increase in the amount of gas which could be injected at a given water flow rate. All exit areas used exhibited a choking phenomena when amounts of gas in excess of the maximum called for by the continuity equations were used. When choking occurred, pressures in the duct were built up and a large amount of spray was expelled from the entrance. It was found that this effect coincided with a leveling off of the gross thrust vs.  $\delta$  curve (figure 10). It is possible that if sufficient gas were injected for a given area ratio and water flow, gross thrust would reach a maximum with increasing  $\delta$ . This condition was not reached experimentally.

In the early experiments much trouble was experienced with uneven performance. This effect was very apparent in the exhaust stream. Pressures were built up at the exit section and expansion took place as the stream left the duct, causing a cone shaped spray exhaust (figure 19). Calculation showed that  $a_m$  in a gas-water mixture was quite low and it was decided to try a de Laval nozzle at the exit.

At low flow rates the de Laval nozzles had no effect on performance as shown in the lower two curves in figure 9. These compare results with and without a de Laval nozzle using  $H_2$  gas and identical flow rates. Effective exhaust velocities were almost identical at all gas flow rates. The exhaust stream was straight with smooth performance and no spray effects.

At high flow rates the nozzles gave a definite increase in performance. The three upper curves in figure 9 give a direct



comparison between two different de Laval nozzles and no nozzle. At low values of  $W_g$ , results were very similar with the curve for no nozzle lying between those with nozzles. At higher values of  $W_g$ , use of the de Laval nozzle gave increased values of  $U_{eff}$ . Exhaust streams were smooth and had no spray effects. Positive thrust was obtained for values of  $W_g > 8 \times 10^{-3}$  lb/sec with effective exhaust velocities of the order of 70,000 ft/sec using hydrogen gas, where effective exhaust velocity is defined as thrust divided by the mass of gas injected per second.

Study of figure 9 shows that increasing water flow rate at a steady gas flow rate increases the effective exhaust velocity. If water flow is maintained constant, increasing the weight rate of gas flow causes a steady decrease in effective exhaust velocity from an initial peak. Thrust however increases with increasing  $W_g$ .

A direct comparison between nitrogen and hydrogen is given in figure 10. Theoretically the two gases should give the same performance for the same volume flow rate. Experimentally  $N_2$  gave better performance than  $H_2$  in all cases.

## CONCLUSIONS

The hydroduct body should consist of three functional parts--a diffuser, a mixing section, and an exit nozzle. The purpose of the diffuser is to convert the dynamic pressure of the water entering the duct to static pressure at the mixing section. At a constant water flow rate, the efficiency of the diffuser determines the pressure in the mixing section, which corresponds to the combustion chamber pressure in a rocket motor. When a large volume of gas is injected into the mixing section, the pressure is increased. This creates a back pressure which tends to prevent separation of flow from the diffuser walls. When the flow separates from the diffuser walls, gas is allowed to escape from the inlet end of the duct. A well designed diffuser, in which the flow does not separate from the walls, prevents this occurrence, except when the chamber pressure is sufficient to overcome the dynamic pressure of the entering stream.

The actual mixing section may be very short, since mixing may take place partly in the diffuser and exit sections. In an actual hydroduct, water reactive chemicals would probably be injected into the duct and gas would be generated in the mixing section. In experimental work it is more convenient to inject gas into the duct through orifices. In order to best approximate theoretical conditions it is desirable to provide the gas well distributed in the water. Turbulence in the mixing section promotes good mixing and improves the performance of the duct.

The diameter of the duct at the mixing section is not critical. Too small a diameter does not allow sufficient pressure recovery; too large a diameter reduces the velocity so that turbulence and good mixing do not occur.

4 The size of gas bubbles as they are injected into the duct has little effect on the performance. However, if the gas coalesces in large bubbles, much of it does not do work on the water and the performance is reduced. When the velocity in the mixing section is below a certain critical value, a large part of the gas injected will rise and collect in the top of the duct. This gas will escape intermittently with a loud popping noise. When this occurs, the thrust will fluctuate rapidly.

For each value of  $\delta$ , there is a theoretical optimum value of  $A_4/A_1$ . If no gas were injected and there were no thrust,  $A_4$  would be equal to  $A_1$ , and  $U_4$  would be equal to  $U_1$ . If gas is injected, then  $A_4$  should be greater than  $A_1$ . At low values of the theoretical optimum value of area ratio gives the highest effective exhaust velocities, but at high values of  $\delta$  the effective exhaust velocities are very nearly the same for different values of the area ratio. The reason for this is that the velocity of sound in the mixture is reached at high values of  $\delta$ . Since this velocity cannot be exceeded in a contracting nozzle, the exit velocity is very nearly the same for all reasonable values of the area ratio, hence the thrust is very nearly constant. The fact that sonic velocity is reached in the exit section

is further borne out by the fact that high pressures are built up at the exit section, causing the mixture to expand after leaving the duct. When a de Laval nozzle is added to the exit section, the thrust is increased and the operation of the duct is noticeably smoother.

For high gas rates, at which positive net thrust is obtained the experimental performance is considerably lower than the theory indicates. As the water rate is increased, the experimental results more nearly approach the theoretical. A water rate higher than any used in these experiments would probably give a further increase in performance.

When a hydroduct is run at high gas rates, the thrust increases monotonically as the volume of gas injected is increased. This is due to the increase in the velocity of sound in the mixture as the gas to water volume ratio is increased. Since the velocity of sound limits the exit velocity which can be obtained with contracting nozzle, the exit velocity can only be increased by using a de Laval nozzle or by increasing the velocity of sound in the mixture. The latter possibility does not seem at all promising, because either the temperature of the gas or the mass ratio of gas to water would have to be increased by a large factor.

The optimum area ratio of a de Laval nozzle is a function

of  $\delta$  and the ratio of the chamber pressure to the ambient pressure. The chamber pressure can be increased by injecting more gas until the pressure in the chamber forces gas out the entrance of the duct. For a well designed diffuser this occurs when the static pressure in the chamber is high enough to overcome the dynamic pressure of the entering stream. In the tests performed the ratio of chamber pressure to ambient pressure was limited to small values, which limited the optimum area ratio of the nozzle used to a still smaller value. The nozzle which gave the best performance in the tests had an area ratio of only 1.26/1.

In order to realize the potentialities of the hydroduct for high speed propulsion, it appears that a means of obtaining high chamber pressures without forcing gas out the entrance must be devised. With a chamber pressure of 600 psi. and an ambient pressure of 20 psi., a de Laval nozzle with an area ratio of 4/1 would be about the optimum. If the necessary chamber pressure could be obtained, such a nozzle would probably give a sufficiently high exhaust velocity to obtain positive thrust considerably greater than that obtained at lower chamber pressure.

DATA FOR HYDROGEN GAS AT 59° F  
AND WATER RATE OF 80.9 Ft/sec.

$\delta$	$M \times 10^4$	$a_m$ (Isothermal) ft/sec.	$a_m$ (Adiabatic) ft/sec.	U 4 ft/sec.
.273	.242	82.5	97.5	86.0
.361	.312	75.0	89.0	87.4
.603	.535	70.0	83.0	91.0
1.060	.950	68.0	80.5	98.4
1.080	.960	67.7	80.3	98.7
1.500	1.350	69.5	82.3	104.0
2.140	1.900	72.1	85.5	114.0
2.330	2.070	74.2	87.8	116.0
4.180	3.720	86.0	102.0	138.0
6.750	6.000	100.0	119.0	164.0
9.000	7.200	107.0	126.0	186.0

$$a_m = a_g \sqrt{\frac{M}{M+1} \frac{1}{\delta}} \left[ 1 + \frac{1}{\delta} \right] \quad \text{for Isothermal case}$$

$$a_m = a_g \sqrt{\frac{M}{M+1} \frac{1}{\delta}} \left[ 1 + \frac{1}{\delta} \right] \quad \text{for Adiabatic case}$$

$$a_g = \sqrt{(1.40)(1718)(14.5)(519)} = 4250 \text{ ft/sec. for } H_2 \text{ gas at } 59^\circ \text{ F.}$$

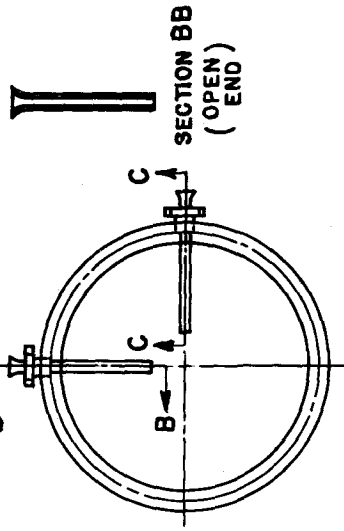
$$a_g = \sqrt{(1.40)(1718) \frac{29}{28} (519)} = 1140 \text{ ft/sec. for } N_2 \text{ gas at } 59^\circ \text{ F.}$$

DATA FOR NITROGEN GAS AT 59° F  
AND WATER RATE OF 80.9 ft./sec.

$\delta$	$M \times 10^4$	$a_m$ (Isothermal)	$a_m$ (Adiabatic)
.293	3.7	82	97
.314	3.9	78	92.3
.450	5.6	73	86.6
.470	5.8	72.5	85.8
.600	7.4	69.6	82.6
1.00	12.5	68.0	80.5
1.44	18.0	68.5	81.0
2.12	26.4	73.1	86.5

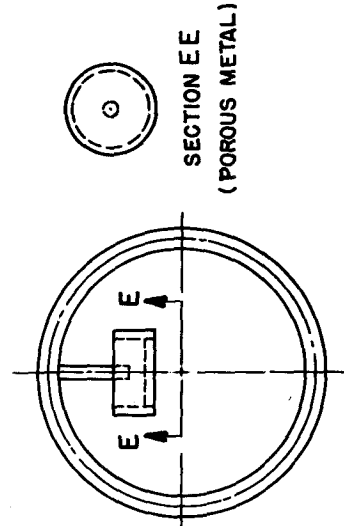
	Gas Reg. Pressure <u>lbs/in.<sup>2</sup></u>	Gas lbs/ <u>sec.</u>	Water lbs/ <u>sec.</u>	Gross Thrust <u>lbs.</u>	Drag <u>lbs.</u>	Net Thrust <u>lbs.</u>	U eff. <u>ft/sec.</u>
H <sub>2</sub> gas							
	20	.001415	16.67	3.6	4.8	-1.2	81,900
1.44" Exit	40	.00296	16.67	4.2	4.8	- .6	45,600
Diameter	60	.00385	16.67	5.1	4.8	+ .3	42,600
No Exp.	80	.00493	16.67	5.8	4.8	+1.0	37,700
Nozzle	100	.00655	16.67	6.4	4.8	+1.6	31,600
1/4" Copp.tubes	120	.00896	16.67	6.8	4.8	+2.0	24,400
Small Holes							
H <sub>2</sub> gas	20	.000762	27.4	4.7	18.0	-13.3	198,000
Exp.Nozzle	40	.00253	27.4	10.2	17.5	- 7.3	130,000
1.44 to 1.75	60	.00370	27.4	14.3	17.5	- 3.2	124,000
1/4" Copp.tub.	80	.00522	27.4	16.3	17.5	- 1.2	101,000
Small Holes	100	.00714	27.4	19.0	19.0	0.0	86,000
	120	.00787	27.4	19.0	19.0	0.0	77,700
	140	.00940	27.4	20.0	19.0	+ 1.0	68,500
N <sub>2</sub> gas	40	.010	27.4	6.7	17.8	-11.1	21,600
1.44 Exit	60	.016	27.4	9.9	17.6	-7.7	20,000
Diameter	80	.021	27.4	11.3	17.5	-6.2	17,300
No. Exp.	100	.023	27.4	11.7	18.5	-6.8	16,400
Nozzle	180	.050	27.4	17.0	17.8	- .8	10,900
1/4" Copp. Tubes							
Small Holes	40	.0107	27.4	7.7	21.5	-13.8	23,200
N <sub>2</sub> gas	60	.0154	27.4	11.7	21.5	- 9.8	23,200
Exp.Nozzle	80	.0204	27.4	13.4	21.5	- 8.1	21,000
1.44 - 1.62	150	.0344	27.4	18.0	21.0	- 3.0	16,900
1/4" Copp.Tubes	200	.0492	27.4	19.5	21.0	- 1.5	12,800
Small Holes	300	.0724	27.4	23.0	21.0	+ 2.0	10,200

FIGURE 1. HYDRODUCT SHAPES AND GAS INJECTION SYSTEMS



SECTION AA

SECTION CC (PERFORATED)



SECTION DD

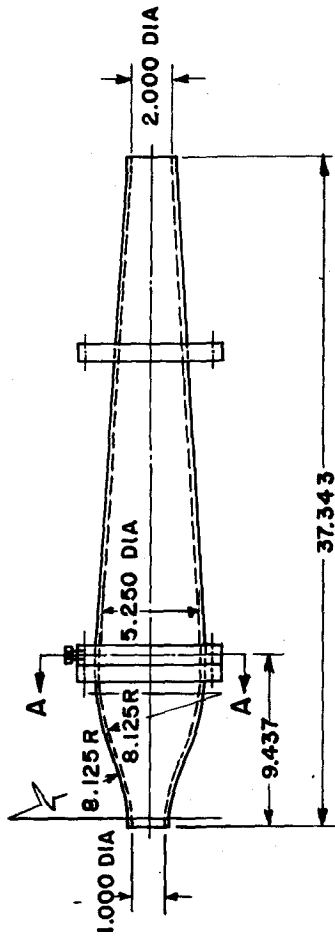


FIGURE 1 a

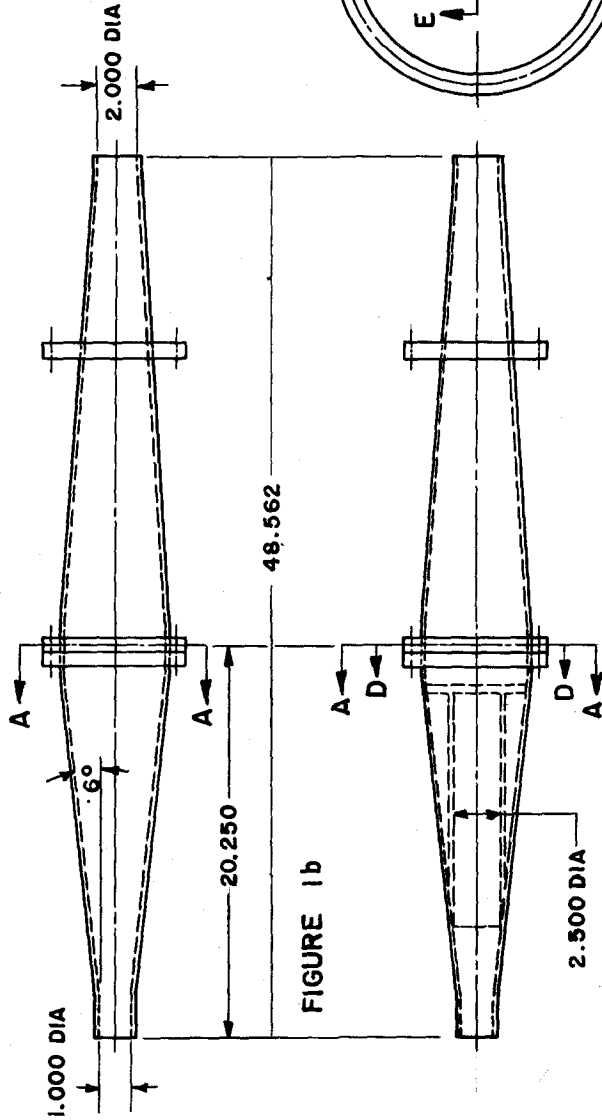


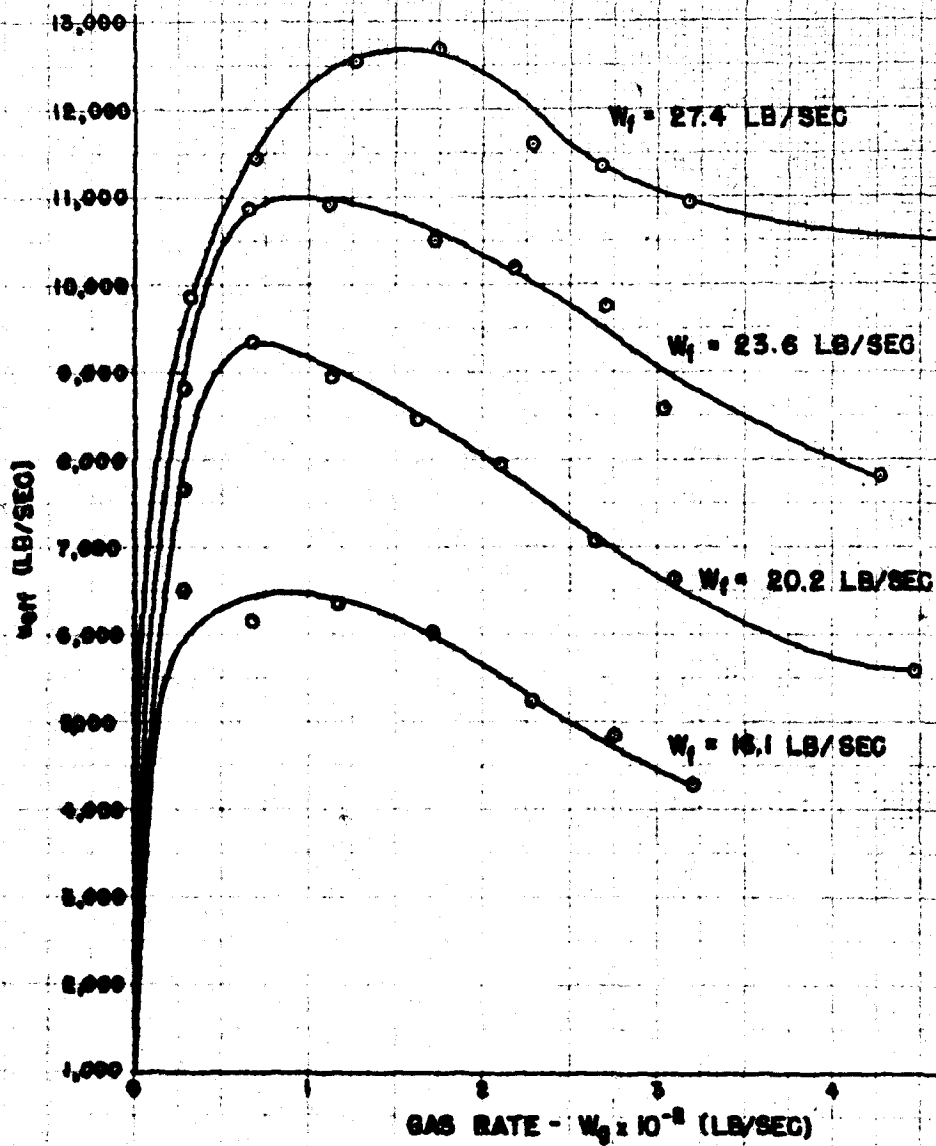
FIGURE 1 b

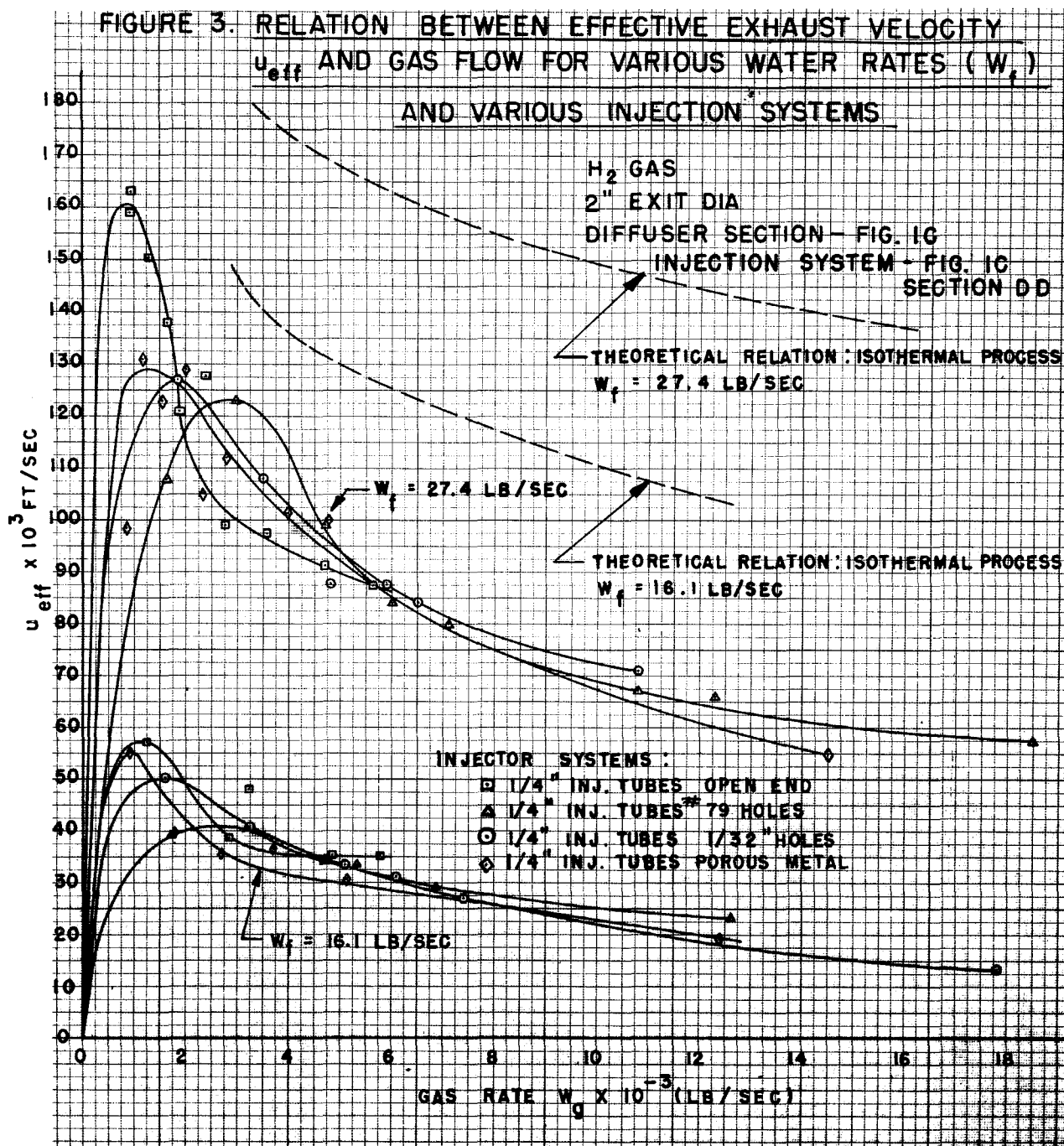
FIGURE 1 c



**FIGURE 2**  
RELATION BETWEEN EFFECTIVE EXHAUST VELOCITY  
( $u_{eff}$ ) AND GAS FLOW FOR VARIOUS WATER RATES ( $W_f$ )

$N_2$  GAS  
 2" EXIT DIAMETER  
 8 INJECTOR TUBES ( $1/32$  IN)  
 WITH GAS INJECTED NORMAL  
 TO FLOW





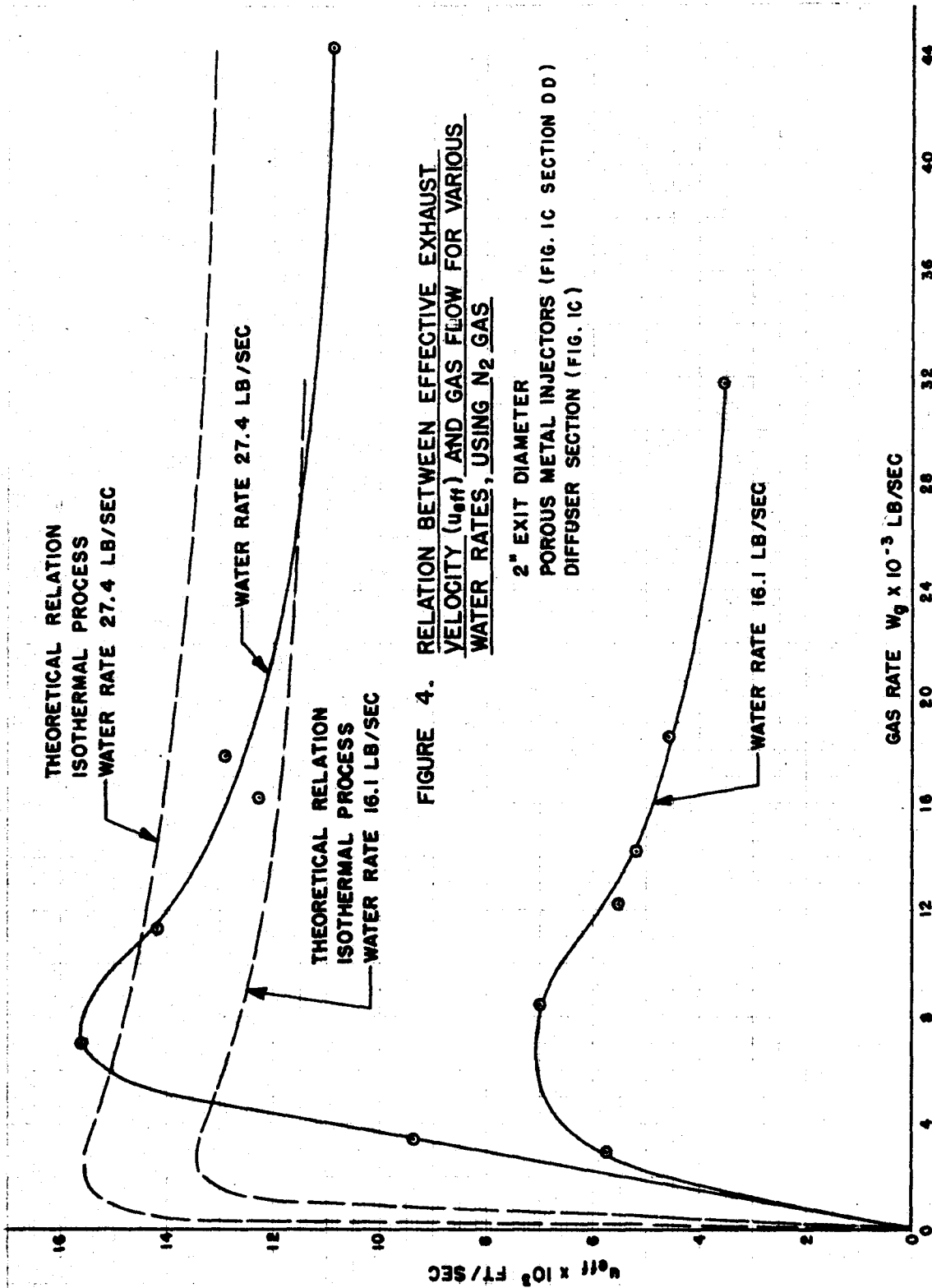
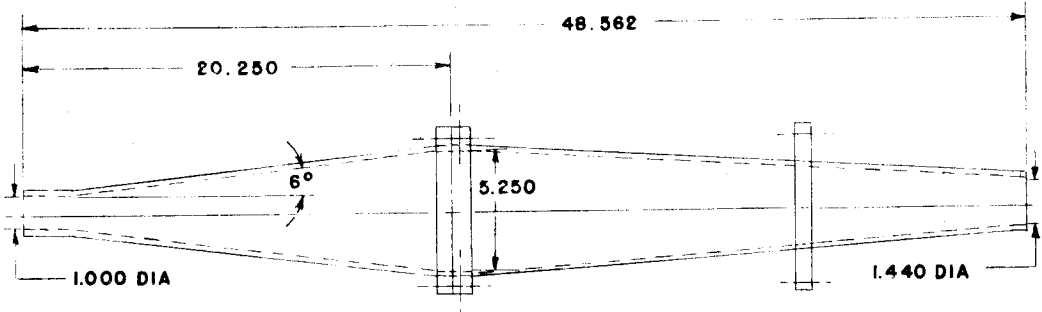


FIGURE 4. RELATION BETWEEN EFFECTIVE EXHAUST VELOCITY ( $u_{eff}$ ) AND GAS FLOW FOR VARIOUS WATER RATES, USING  $N_2$  GAS

2" EXIT DIAMETER  
POROUS METAL INJECTORS (FIG. 1C SECTION DD)  
DIFFUSER SECTION (FIG. 1C)



HYDRODUCT SHAPE A

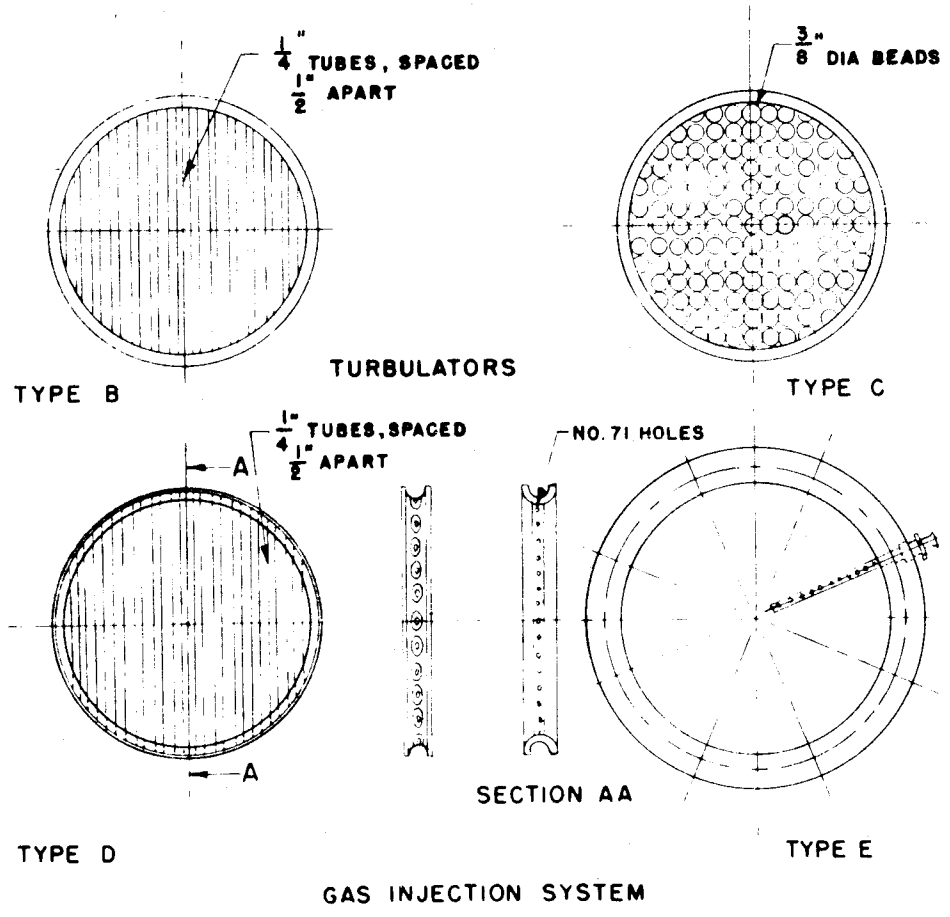


FIGURE 5  
HYDRODUCT SHAPE, TURBULATOR, AND  
GAS INJECTION SYSTEM

FIGURE 6. RELATION BETWEEN EFFECTIVE EXHAUST VELOCITY ( $u_{eff}$ )  
AND GAS RATE, USING  $H_2$  GAS

WATER RATE = 27.4 LB/SEC  
HYDRODUCT SHAPE, FIGURE 5

THEORETICAL RELATION  
ISOTHERMAL PROCESS

- TURBULATOR, TYPE C, FIGURE 5
- ▲ GAS INJECTION SYSTEM, TYPE E, FIGURE 5
- ▲ TURBULATOR, TYPE B, FIGURE 5
- ▲ GAS INJECTION SYSTEM, TYPE E, FIGURE 5
- TURBULATOR, TYPE C, FIGURE 5
- GAS INJECTION SYSTEM, TYPE D, FIGURE 5

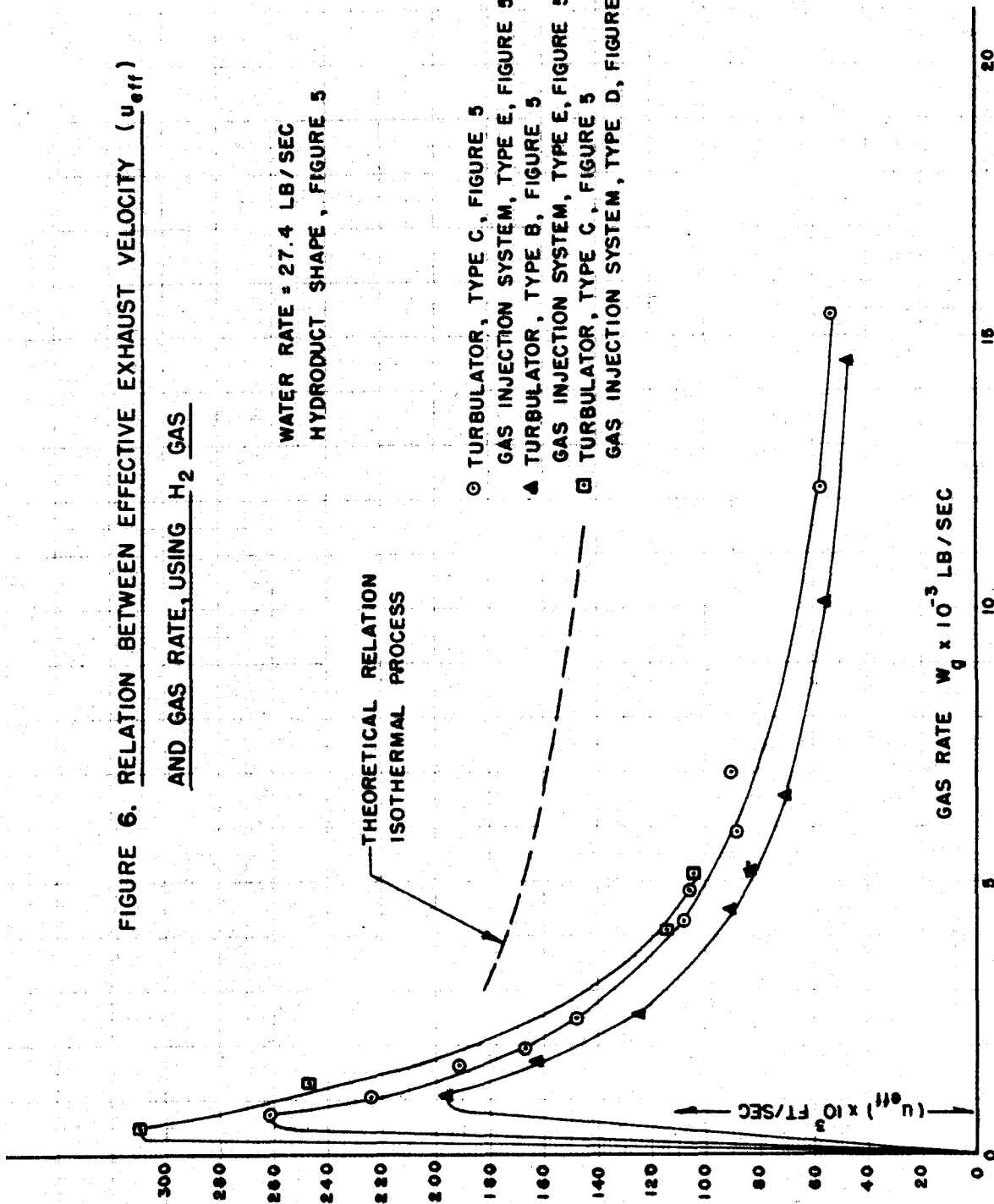
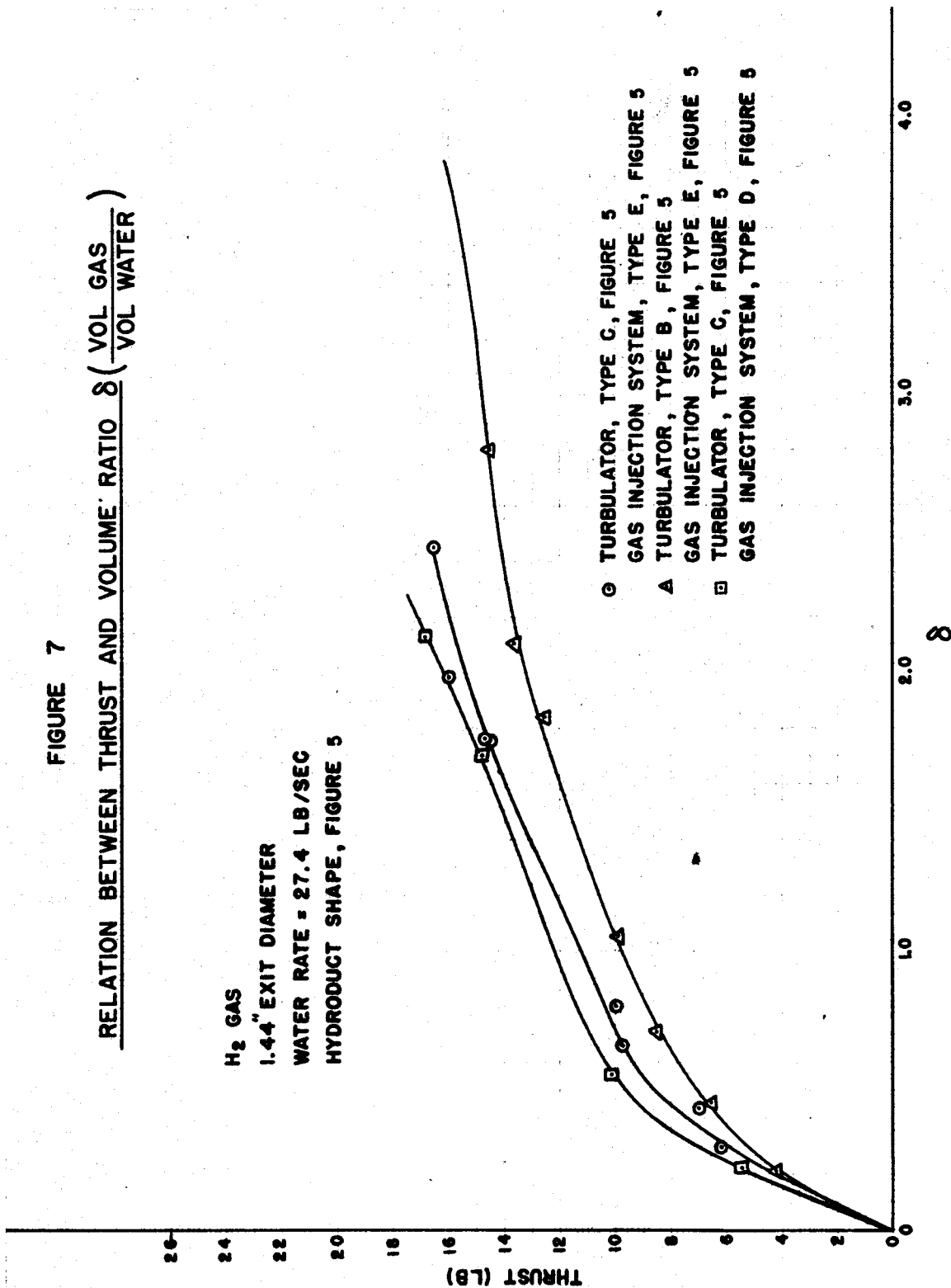
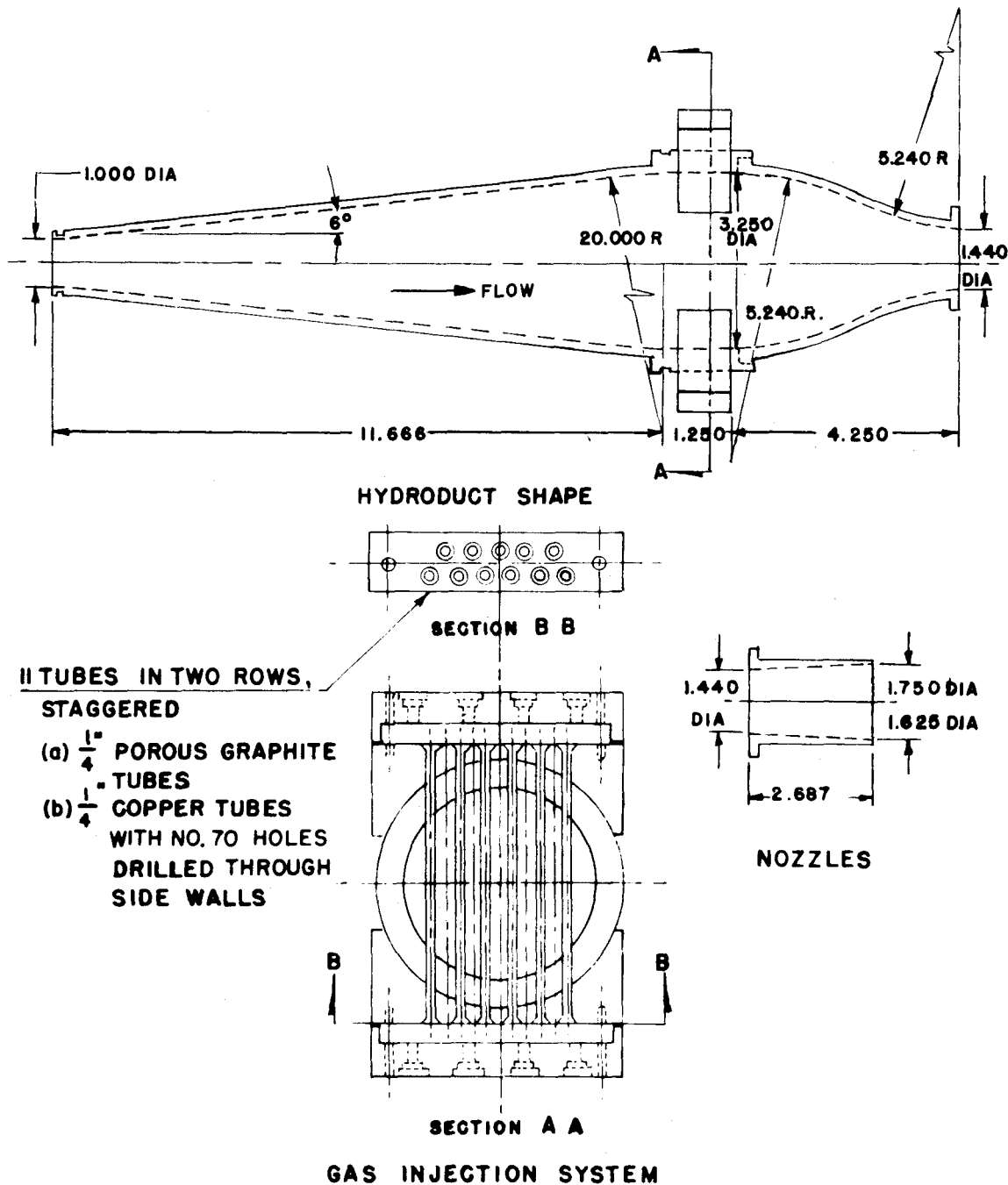


FIGURE 7

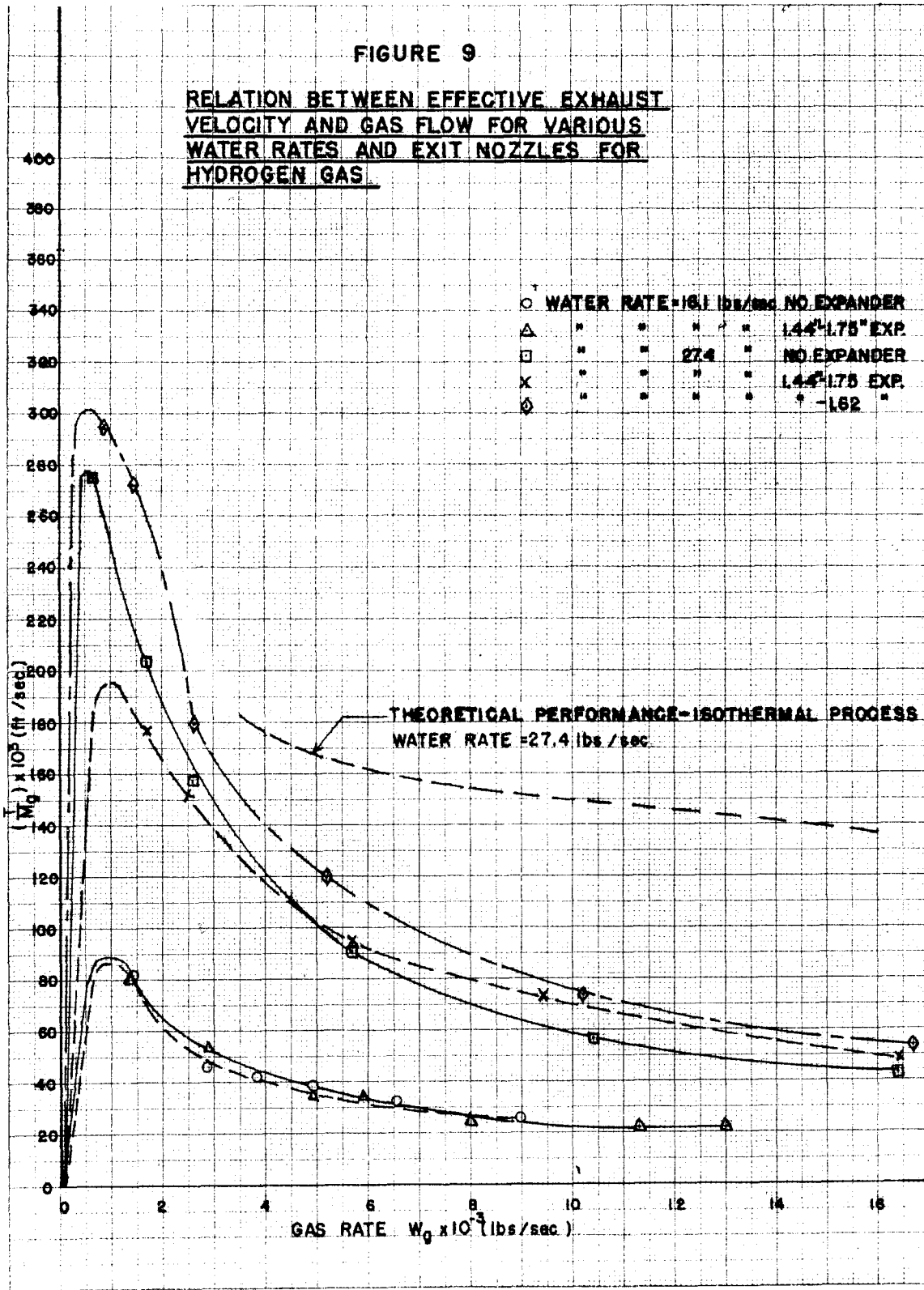
RELATION BETWEEN THRUST AND VOLUME RATIO  $\delta$  ( $\frac{\text{VOL GAS}}{\text{VOL WATER}}$ )

H<sub>2</sub> GAS  
1.44" EXIT DIAMETER  
WATER RATE = 27.4 LB/SEC  
HYDRODUCT SHAPE, FIGURE 5

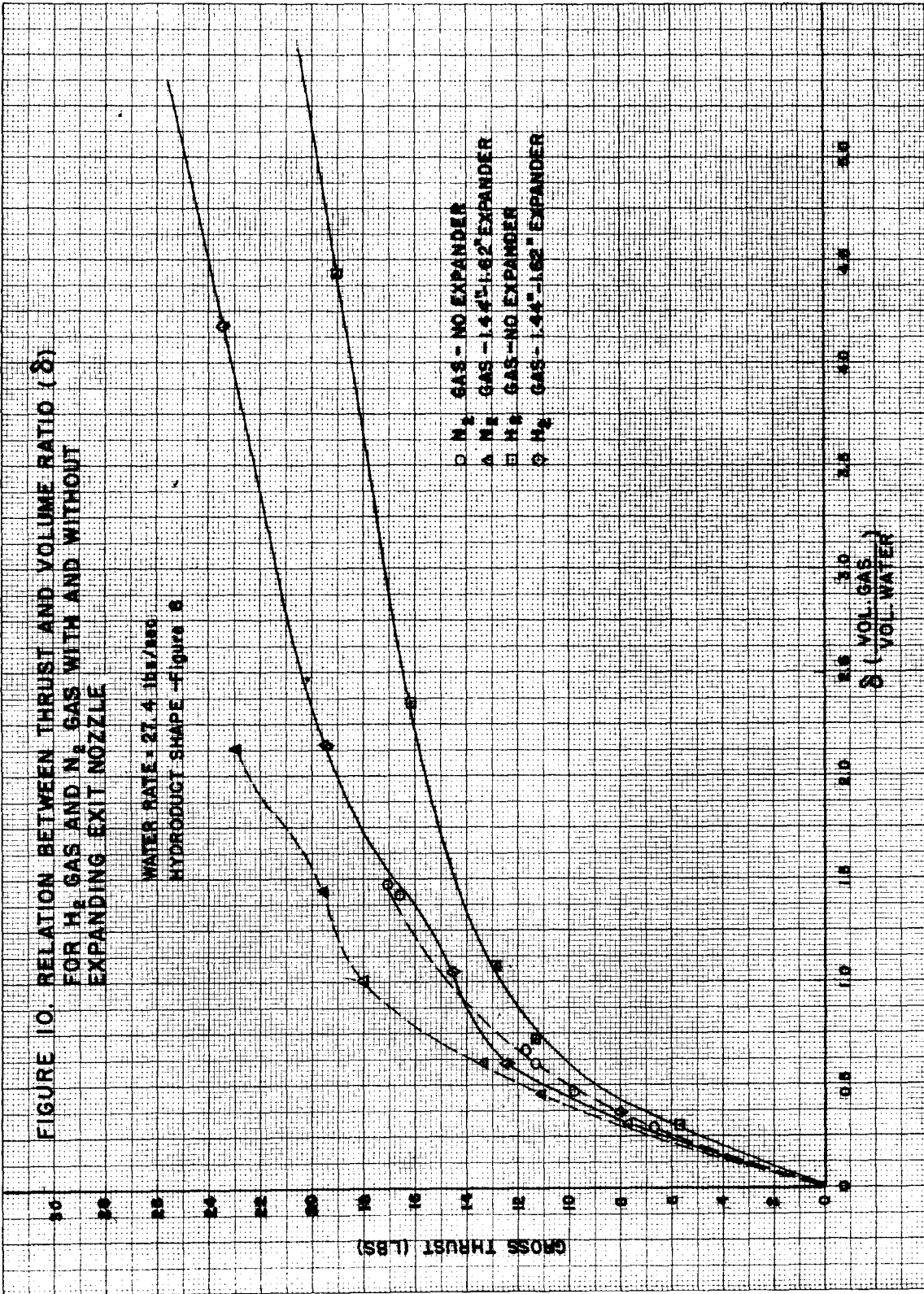


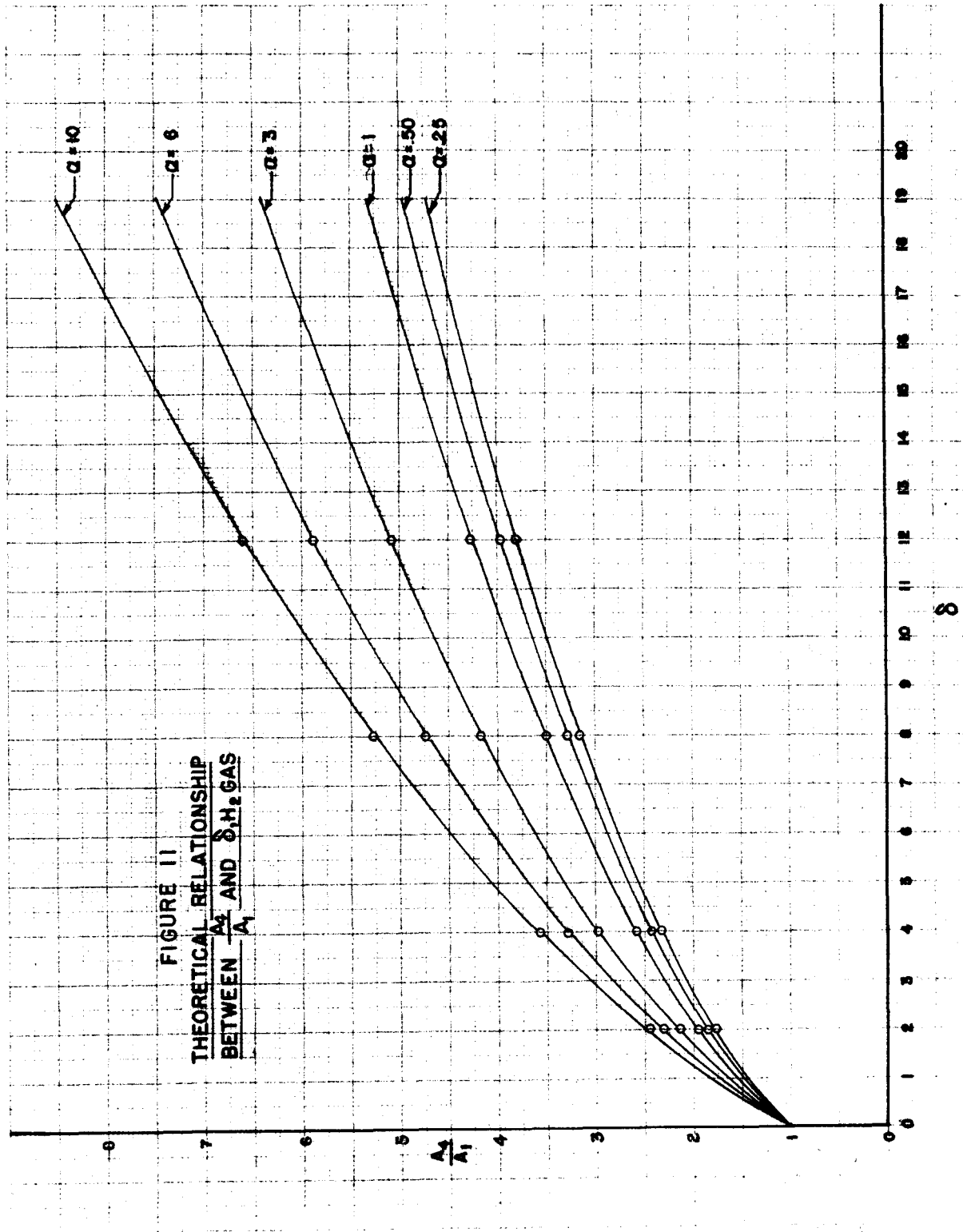


**FIGURE 8. HYDRODUCT SHAPE, GAS INJECTION SYSTEM, AND NOZZLES**









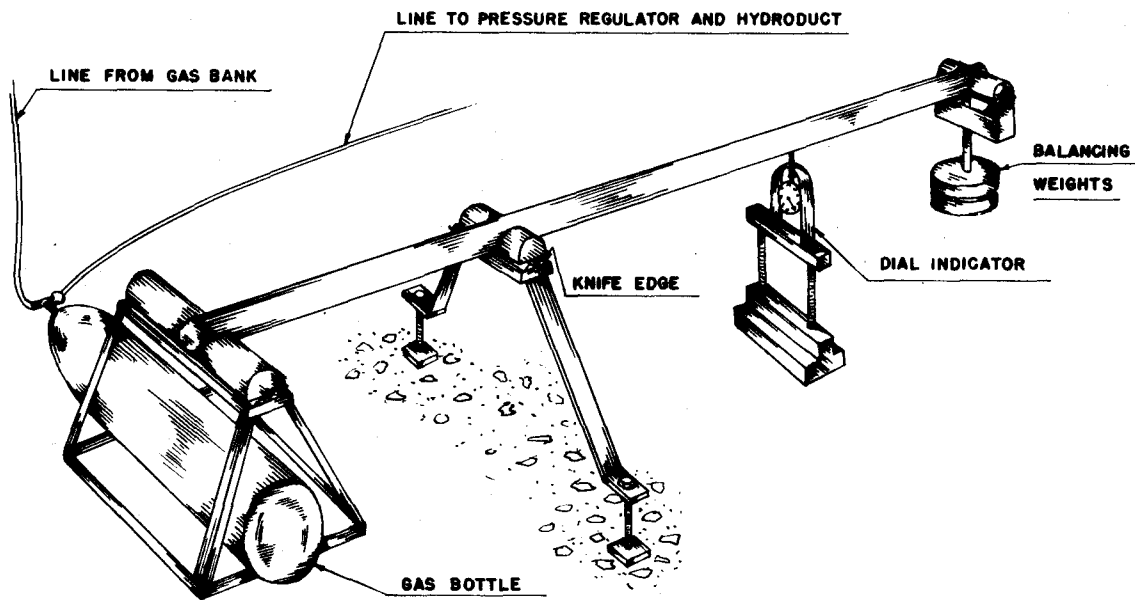
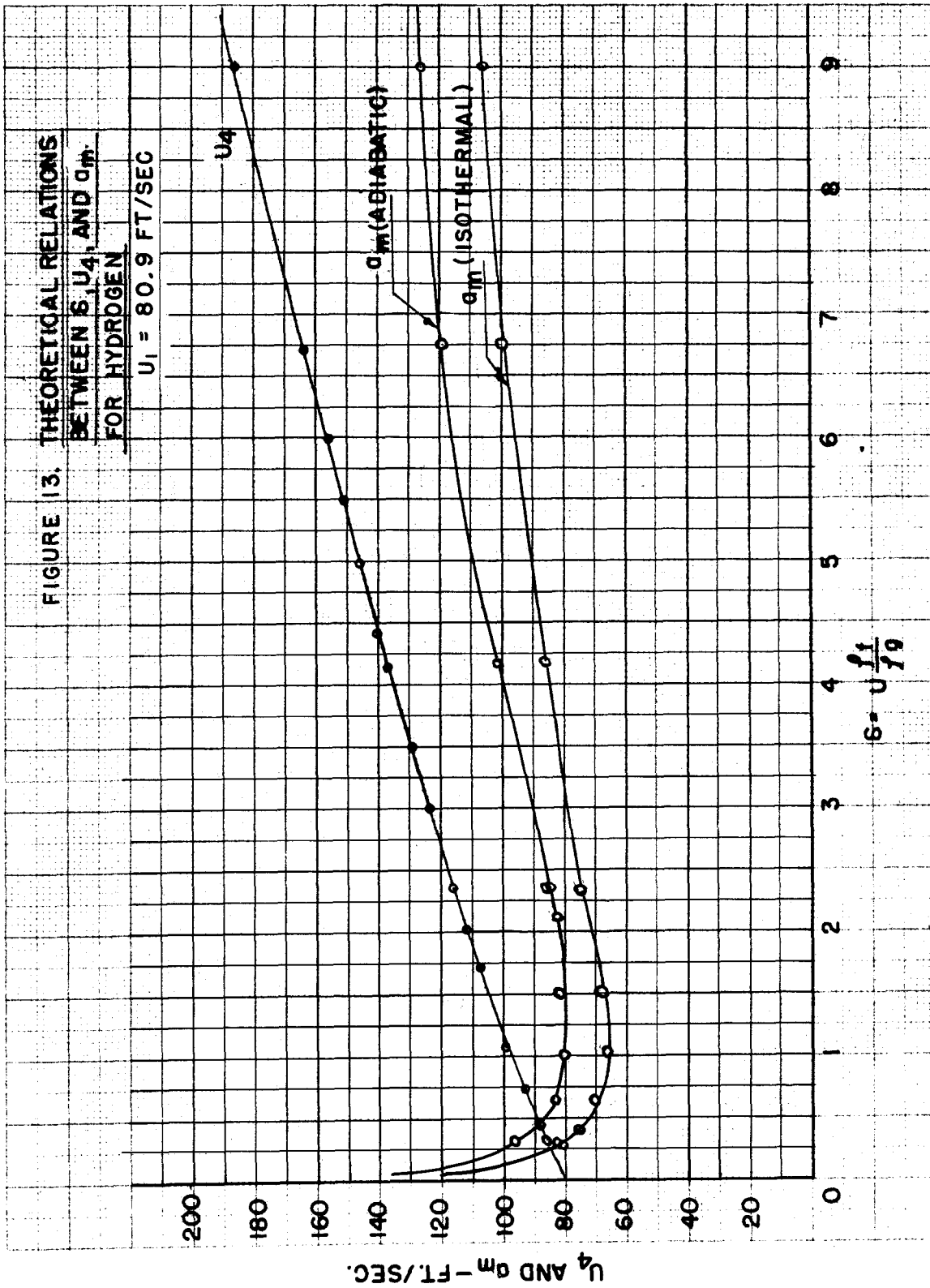


FIGURE 12. GAS-WEIGHING DEVICE

FIGURE 13. THEORETICAL RELATIONS  
BETWEEN  $U_4$ ,  $U_3$ , AND  $\alpha_m$   
FOR HYDROGEN

$U_1 = 80.9$  FT/SEC





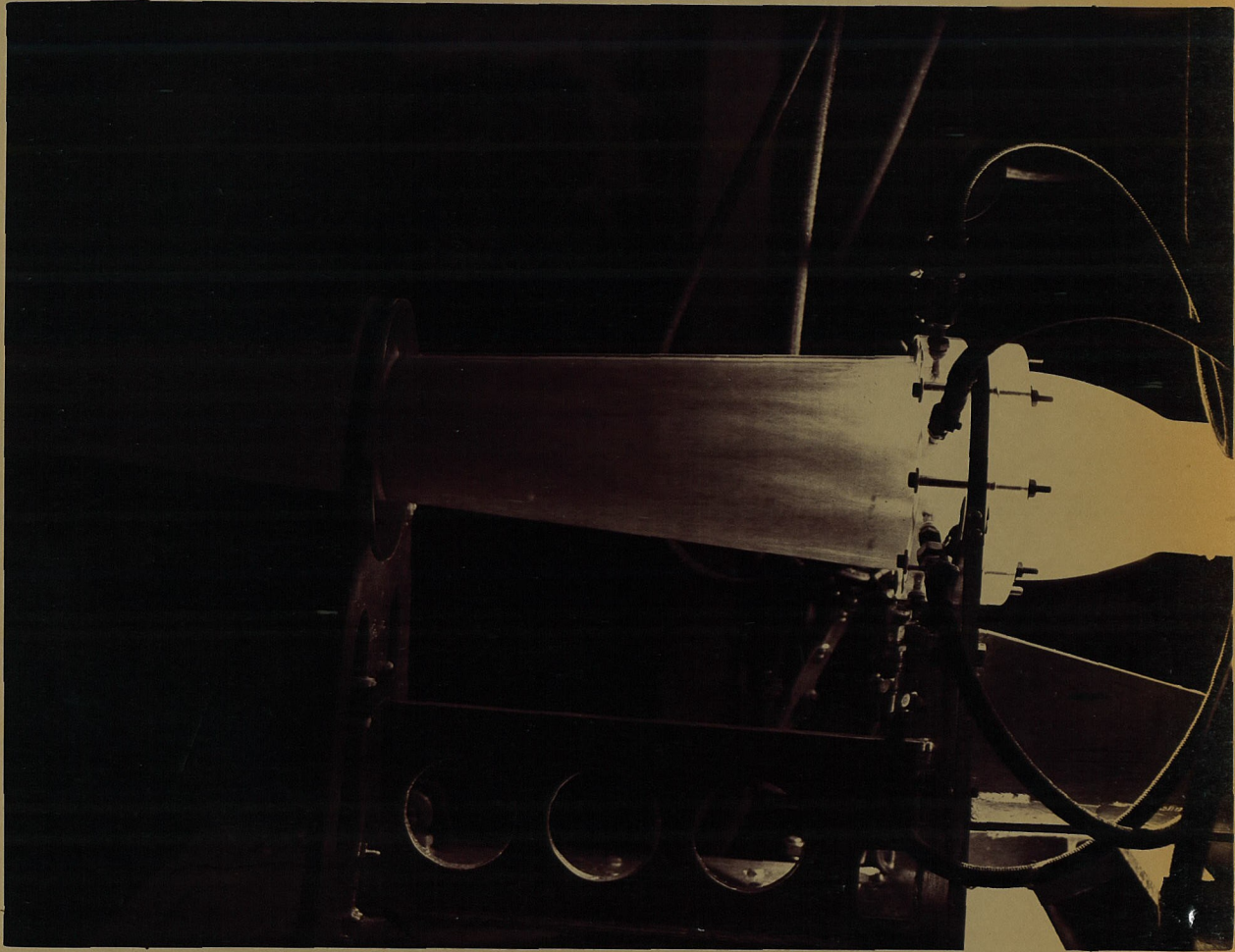


FIGURE 14. FIRST DESIGN, LOW FLOW RATE



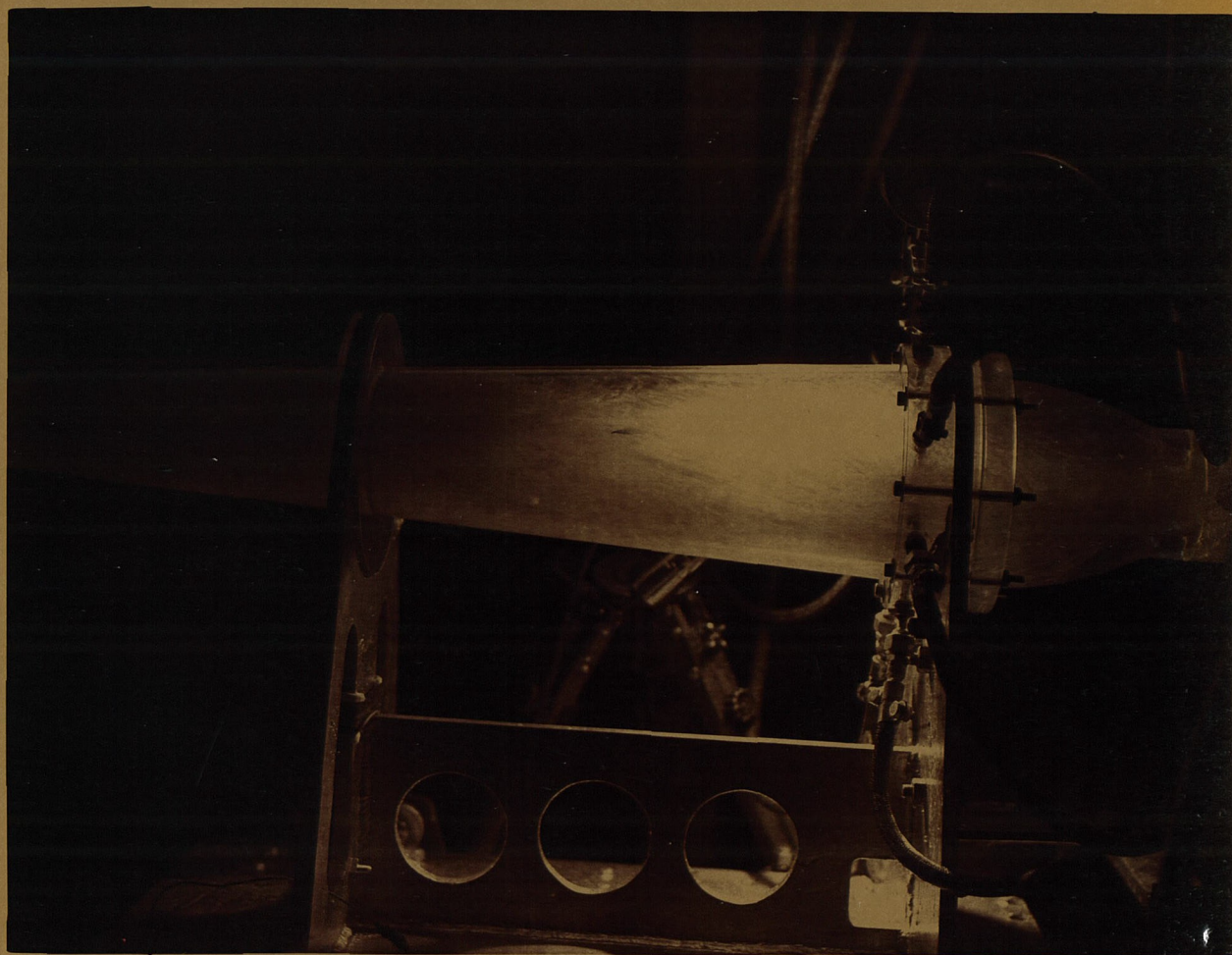


FIGURE 15. FIRST DESIGN, HIGH FLOW RATE





FIGURE 16. EXIT SECTION SHOWING DISTRIBUTION OF GAS  
IN MIXTURE





FIGURE 17. EXHAUST STREAM



~~CLASSIFICATION cancelled~~

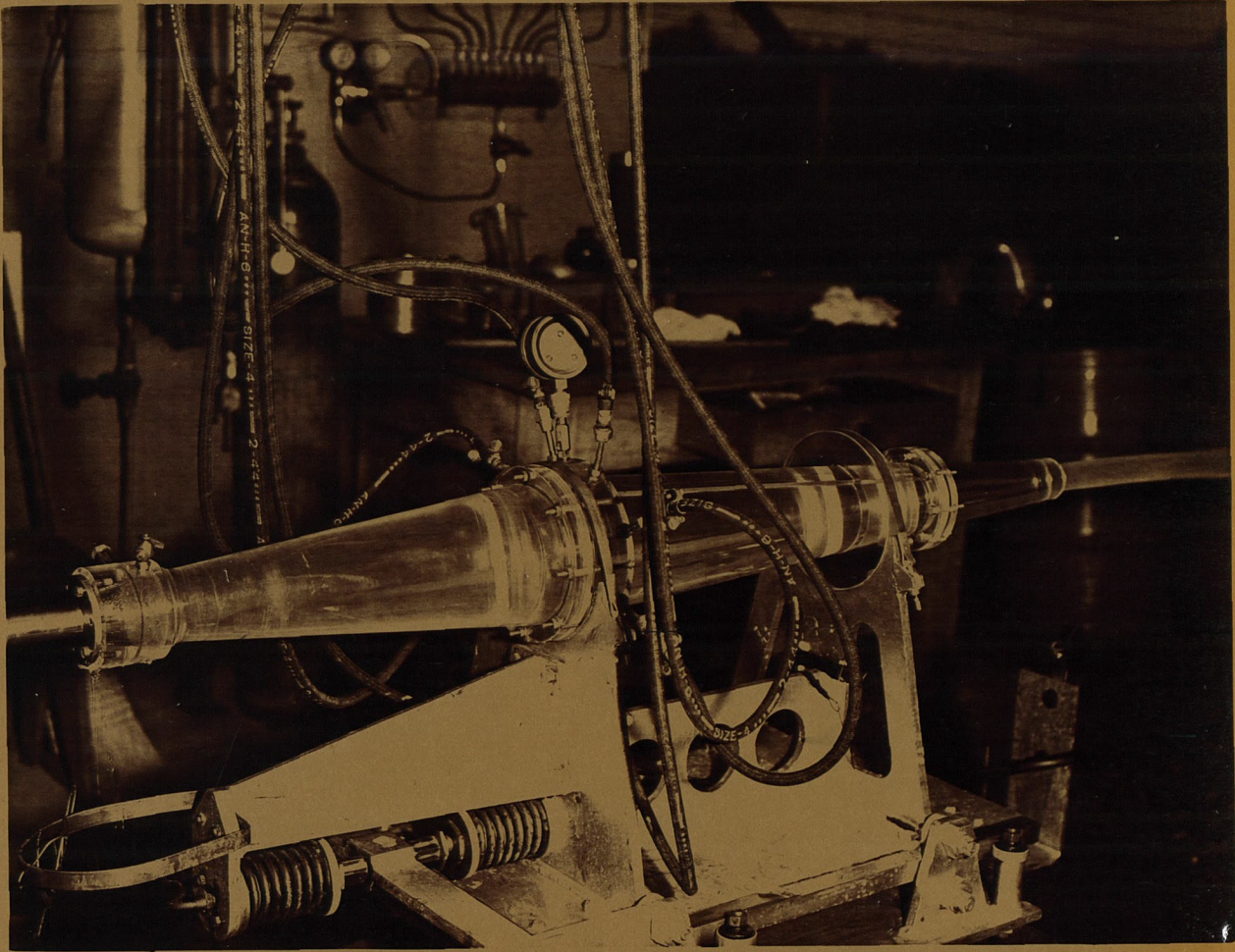


FIGURE 18. SECOND DESIGN, WATER FLOW ESTABLISHED

~~CLASSIFICATION cancelled~~



~~CLASSIFICATION cancelled~~

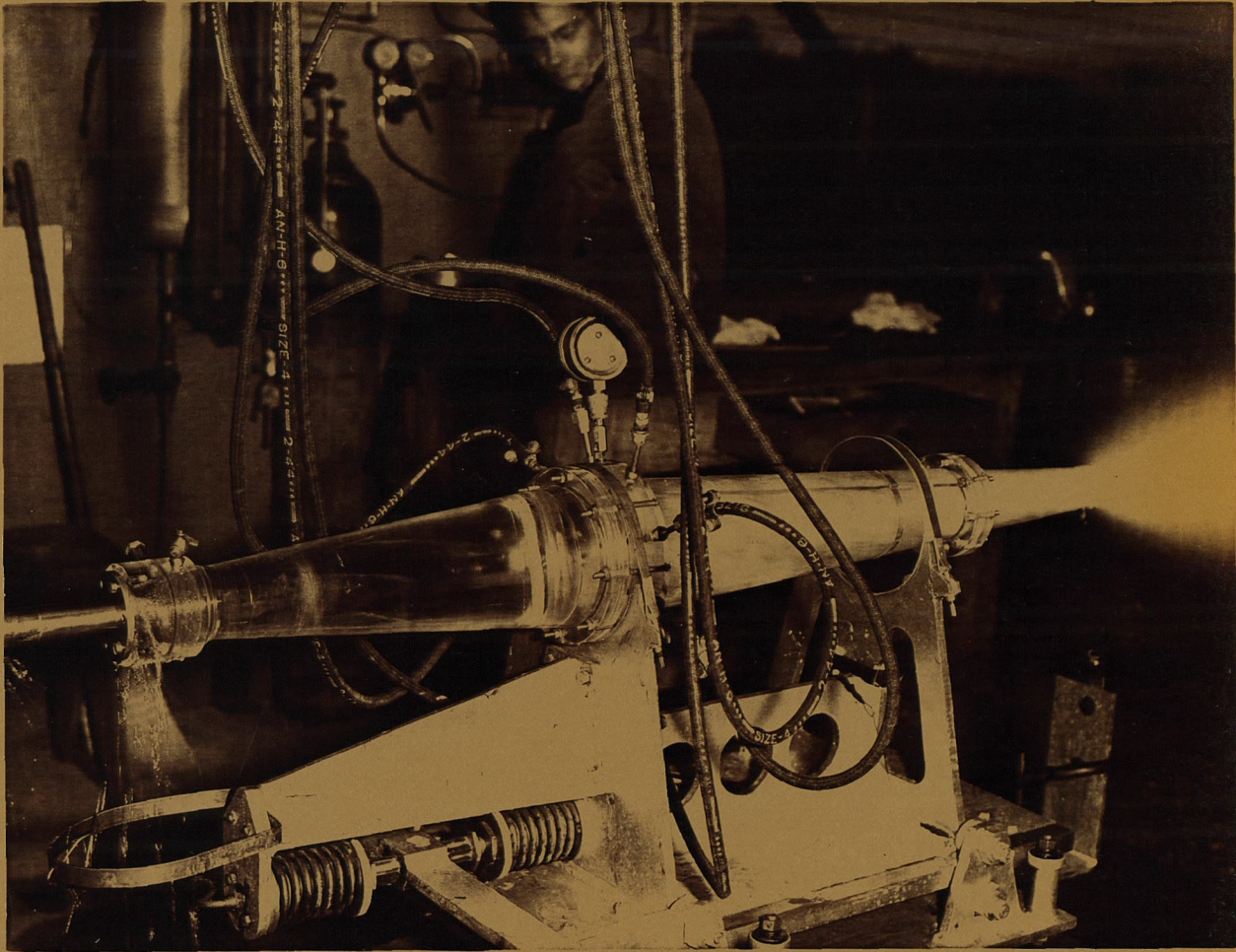


FIGURE 19. SECOND DESIGN , MIXTURE OF GAS AND WATER

~~CLASSIFICATION cancelled~~